Wave Motion 76 (2018) 9–18

Contents lists available at ScienceDirect

Wave Motion

journal homepage: www.elsevier.com/locate/wamot

Gain–loss-driven travelling waves in PT-symmetric nonlinear metamaterials

M. Agaoglou [a,d,*], M. Fečkan [b,c], M. Pospíšil [b,c], V.M. Rothos [d], H. Susanto [e]

[a] Department of Mathematics and Statistics, University of Massachusetts, Lederle Graduate Research Tower, Amherst, MA 01003, USA
[b] Department of Mathematical Analysis and Numerical Mathematics, Comenius University in Bratislava, Mlynská dolina, 842 48 Bratislava, Slovakia
[c] Mathematical Institute of Slovak Academy of Sciences, Štefánikova 49, 814 73 Bratislava, Slovakia
[d] Lab of Nonlinear Mathematics and Department of Mechanical Engineering, Faculty of Engineering, Aristotle University of Thessaloniki, Thessaloniki 54124, Greece
[e] Department of Mathematical Sciences, University of Essex, Wivenhoe Park, Colchester CO4 3SQ, United Kingdom

HIGHLIGHTS

- A one-dimensional model of nonlinear magnetic metamaterials with parity-time-symmetric potentials is considered.
- The existence of localized travelling waves is obtained by performing a Melnikov function analysis.
- Direct numerical computations are performed showing good agreement with the analysis.
- A snaking structure in the bifurcation diagram can be obtained.

ARTICLE INFO

Article history:
Received 30 April 2017
Received in revised form 21 August 2017
Accepted 17 October 2017

Keywords:
PT-Symmetry
Melnikov theory
Nonlinear metamaterials
Homoclinic snaking

ABSTRACT

In this work we investigate a one-dimensional parity-time (PT)-symmetric magnetic metamaterial consisting of split-ring dimers having gain or loss. Employing a Melnikov analysis we study the existence of localized travelling waves, i.e. homoclinic or heteroclinic solutions. We find conditions under which the homoclinic or heteroclinic orbits persist. Our analytical results are found to be in good agreement with direct numerical computations. For the particular nonlinearity admitting travelling kinks, numerically we observe homoclinic snaking in the bifurcation diagram. The Melnikov analysis yields a good approximation to one of the boundaries of the snaking profile.

1. Introduction

Metamaterials are composite materials that are engineered structurally (rather than chemically) to have exotic properties that may not be found in nature. They are artificial materials made of "artificial atoms" (called meta-atoms) that are placed periodically. Together with the properties of the "atoms", the geometry (e.g., the perfectly periodic arrangement) then creates non-natural, but desirable effective behaviours. The development of this new type of materials was due to the work of Pendry [1,2], following the proposal of Veselago [3] on negative refraction. While Veselago studied continuous systems in his pioneering article, Pendry, on the other hand, started from discrete systems that lead to metamaterials [4]. Because Pendry

* Corresponding author at: Department of Mathematics and Statistics, University of Massachusetts, Lederle Graduate Research Tower, Amherst, MA 01003, USA.
E-mail addresses: agaoglou@math.umass.edu (M. Agaoglou), Michal.Feckan@fmph.uniba.sk (M. Fečkan), michal.pospisil@mat.savba.sk (M. Pospíšil), rothos@auth.gr (V.M. Rothos), hsusanto@essex.ac.uk (H. Susanto).

https://doi.org/10.1016/j.wavemoti.2017.10.003
0165-2125/

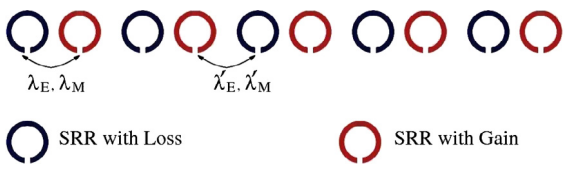

Fig. 1. Schematic of a PT-symmetric metamaterial. The separation between SRRs can be modulated according to a binary pattern (i.e., PT dimer chain). The parameters λ_M, λ'_M and λ_E, λ'_E denote the magnetic (subscript M) and electric (subscript E) interactions between the rings. The sketch is adapted from [9].

considered a mean field (i.e., homogenization) approach that lead him to the findings, certain conditions on the wavelength and the characteristic length of metamaterials should hold in order to validate the description.

Another paradigm of artificial materials is the parity-time (PT) symmetric systems that belong to a class of synthetic materials that do not obey separately the parity (P) and time (T) symmetries but instead they do exhibit a combined PT-symmetry. The ideas and notions of PT-symmetric systems have originated from the extension of ordinary Quantum Mechanics to PT-symmetric (i.e., non-Hermitian) Hamiltonians that have been studied for many years. Recently it has been realized that many classical systems are PT-symmetric [5]. Subsequently, the notion of PT-symmetry has been extended to dynamical lattices, particularly in optics [6,7]. It was immediately after that the theory evolved to include nonlinear lattices [8]. Building metamaterials with PT-symmetry, relying on a delicate balance between gain and loss where loss may be matched with an equal amount of gain, may provide a way out from high losses typically present in many cases and result in altogether new functionalities and electromagnetic characteristics [9].

Consider a one-dimensional array of dimers, each comprising two nonlinear split-ring resonators (SRRs): one with loss and the other with an equal amount of gain as sketched in Fig. 1. The SRRs are coupled magnetically and/or electrically through dipole–dipole forces [10–13] and are regarded as RLC circuits, featuring a resistance R, an inductance L, and a capacitance C. A tunnel (Esaki) diode forms a nonlinear metamaterial element with gain. The diodes exhibit a well-defined negative resistance region in their current–voltage characteristics that has a characteristic "N" shape. A bias voltage applied to the diode can move its operation point in the negative resistance region and then the SRR-diode system gains energy from the source. The presence of these elements, in addition to providing gain also introduces nonlinearity in the metamaterial.

The alternating magnetic field induces an electromotive force in each SRR due to Faraday's law which in turn produces currents that couple the SRRs magnetically through their mutual inductance. The coupling strength between SRRs is rather weak due to the nature of their interaction (magnetoinductive), and has been calculated accurately [10,13]. The SRRs may also be coupled electrically through the electric dipoles that develop in their slits. Thus, in the general case one has to consider both magnetic and electric coupling between SRRs. However, for particular relative orientations of the SRR slits the magnetic interaction is dominant, while the electric interaction can be neglected in a first approximation [11,12,14]. Here, we study the case where the electric interaction, that depends on the distance of the gaps, is not neglected, see Fig. 1. In our case we take the gaps looking at the same direction.

In the equivalent circuit model picture (see, e.g., [13,15–17]), extended for the PT dimer chain, the dynamics of the charge q_n in the capacitor of the nth SRR is governed by

$$\begin{aligned} &\ddot{q}_{2n+1} + q_{2n+1} + \lambda'_M \ddot{q}_{2n} + \lambda_M \ddot{q}_{2n+2} + \lambda'_E q_{2n} + \lambda_E q_{2n+2} \\ &\quad = \varepsilon \sin(pn + \Omega t) - a q_{2n+1}^2 - \beta q_{2n+1}^3 - \gamma \dot{q}_{2n+1}, \\ &\ddot{q}_{2n+2} + q_{2n+2} + \lambda_M \ddot{q}_{2n+1} + \lambda'_M \ddot{q}_{2n+3} + \lambda_E q_{2n+1} + \lambda'_E q_{2n+3} \\ &\quad = \varepsilon \sin(pn + \Omega t) - a q_{2n+2}^2 - \beta q_{2n+2}^3 + \gamma \dot{q}_{2n+2}, \end{aligned} \tag{1.1}$$

where λ_M, λ'_M and λ_E, λ'_E are the magnetic and electric interaction coefficients, respectively, between nearest neighbours, a and β are nonlinear coefficients, γ is the gain or loss coefficient ($\gamma > 0$), ε is the amplitude of the external driving voltage, while Ω is the driving frequency normalized to $\omega_0 = 1/\sqrt{LC_0}$ and t temporal variable normalized to ω_0^{-1}, with C_0 being the linear capacitance.

Replacing $q_{2n+1} = U_n$ and $q_{2n+2} = V_n$ into (1.1), we obtain

$$\begin{aligned} &\ddot{U}_n + U_n + a U_n^2 + \beta U_n^3 \\ &= -\lambda'_M \ddot{V}_{n-1} - \lambda_M \ddot{V}_n - \lambda'_E V_{n-1} - \lambda_E V_n - \gamma \dot{U}_n + \varepsilon \sin(pn + \Omega t), \\ &\ddot{V}_n + V_n + a V_n^2 + \beta V_n^3 \\ &= -\lambda_M \ddot{U}_n - \lambda'_M \ddot{U}_{n+1} - \lambda_E U_n - \lambda'_E U_{n+1} + \gamma \dot{V}_n + \varepsilon \sin(pn + \Omega t). \end{aligned} \tag{1.2}$$

Looking for travelling waves and hence setting $z = pn + \Omega t$, $U(z) = U_n(t)$, $V(z) = V_n(t)$, (1.2) becomes

$$\begin{aligned} &\Omega^2 U_{zz}(z) + U(z) + a U^2(z) + \beta U^3(z) \\ &= -\lambda'_M \Omega^2 V_{zz}(z-p) - \lambda_M \Omega^2 V_{zz}(z) - \lambda'_E V(z-p) - \lambda_E V(z) - \gamma \Omega U_z(z) + \varepsilon \sin z, \\ &\Omega^2 V_{zz}(z) + V(z) + a V^2(z) + \beta V^3(z) \\ &= -\lambda_M \Omega^2 U_{zz}(z) - \lambda'_M \Omega^2 U_{zz}(z+p) - \lambda_E U(z) - \lambda'_E U(z+p) + \gamma \Omega V_z(z) + \varepsilon \sin z. \end{aligned} \tag{1.3}$$

Our work is concerned with the existence and persistence of localized travelling waves of (1.3). This paper extends our previous studies [18,19], where the persistence of localized travelling waves in a single equation was considered. In the context of PT-symmetric metamaterials, our work extends that of [9] that demonstrated numerically the existence of standing, highly-localized solutions.

This paper is organized as follows. In Section 2 we introduce a Melnikov analysis related to homoclinic motion in the system and study two different cases for different values of our nonlinear coefficients a and β. In Section 3, we present numerical computations comparing the analytical results in the preceding section. Finally, Section 4 summarizes our findings.

2. Melnikov analysis

In this section we perform a Melnikov analysis for homoclinic type motions of (1.3) for weak coupling, forcing and damping, which is expressed after scaling $\lambda_M \to \varepsilon\lambda_M$, $\lambda'_M \to \varepsilon\lambda'_M$, $\lambda_E \to \varepsilon\lambda_E$, $\lambda'_E \to \varepsilon\lambda'_E$, and $z \to z/\Omega$ as

$$\begin{aligned} &U_{zz}(z) + U(z) + aU^2(z) + \beta U^3(z) \\ &= \varepsilon(-\lambda'_M V_{zz}(z-p) - \lambda_M V_{zz}(z) - \lambda'_E V(z-p) - \lambda_E V(z) - \gamma U_z(z) + \sin\Omega z), \\ &V_{zz}(z) + V(z) + aV^2(z) + \beta V^3(z) \\ &= \varepsilon(-\lambda_M U_{zz}(z) - \lambda'_M U_{zz}(z+p) - \lambda_E U(z) - \lambda'_E U(z+p) + \gamma V_z(z) + \sin\Omega z), \end{aligned} \tag{2.1}$$

where the parameter $|\varepsilon| \ll 1$ indicates the perturbative character in the above equations. For $\varepsilon = 0$ the unperturbed system is

$$\begin{aligned} &U_{zz}(z) + U(z) + aU^2(z) + \beta U^3(z) = 0, \\ &V_{zz}(z) + V(z) + aV^2(z) + \beta V^3(z) = 0. \end{aligned} \tag{2.2}$$

We consider the following cases: a) $a < 0$ and $\beta = 0$, and b) $a = 0$ and $\beta = -1$, which represent systems with non-topological and topological localized waves.

2.1. Case (a)

Both equations of (2.2) have a hyperbolic equilibrium $(\overline{p}_i, \overline{q}_i) = \left(0, -\frac{1}{a}\right)$, $i = 1, 2$ where $i = 1$ and $i = 2$ refer to the first and second equation of (2.2), $q_1 = U$, $q_2 = V$, connected by a homoclinic solution

$$p_i = \dot{q}_i, \quad q_i(z) = -\frac{1}{a} + \frac{3\,\mathrm{sech}^2\frac{z}{2}}{2a}.$$

So in the full space $\mathbb{R}^4$, the system (2.2) has a hyperbolic equilibrium

$$(\overline{p}_1, \overline{q}_1, \overline{p}_2, \overline{q}_2)$$

connected by the homoclinic trajectory

$$\begin{aligned} &(p_{1h}(z), q_{1h}(z), p_{2h}(z), q_{2h}(z)) \\ &= \left(-\frac{3\,\mathrm{sech}^2\frac{z}{2}\tanh\frac{z}{2}}{2a}, -\frac{1}{a} + \frac{3\,\mathrm{sech}^2\frac{z}{2}}{2a}, -\frac{3\,\mathrm{sech}^2\frac{z}{2}\tanh\frac{z}{2}}{2a}, -\frac{1}{a} + \frac{3\,\mathrm{sech}^2\frac{z}{2}}{2a}\right). \end{aligned} \tag{2.3}$$

To study the persistence of homoclinic type solutions for (2.1), we compute the Melnikov integrals (for higher dimensions Melnikov analysis see [20–23]). After introducing real parameters τ_1, τ_2 determining the position on the homoclinic type orbits, we derive

$$\begin{aligned} M_1(\tau_1, \tau_2) &:= \int_{-\infty}^{\infty} p_{1h}(z-\tau_1)[-\lambda'_M \dot{p}_{2h}(z-\tau_2-p) - \lambda_M \dot{p}_{2h}(z-\tau_2) \\ &\quad -\lambda'_E q_{2h}(z-\tau_2-p) - \lambda_E q_{2h}(z-\tau_2) - \gamma p_{1h}(z-\tau_1) + \sin\Omega z]dz, \\ M_2(\tau_1, \tau_2) &:= \int_{-\infty}^{\infty} p_{2h}(z-\tau_2)\big[-\lambda_M \dot{p}_{1h}(z-\tau_1) - \lambda'_M \dot{p}_{1h}(z-\tau_1+p) \\ &\quad -\lambda_E q_{1h}(z-\tau_1) - \lambda'_E q_{1h}(z-\tau_1+p) + \gamma p_{2h}(z-\tau_2) + \sin\Omega z\big]\,dz. \end{aligned}$$

We see that the above Melnikov functions have the forms

$$\begin{aligned} M_1(\tau_1, \tau_2) &= M_{11}(\tau_1 - \tau_2) + M_{12}\cos\Omega\tau_1, \\ M_2(\tau_1, \tau_2) &= M_{21}(\tau_1 - \tau_2) + M_{22}\cos\Omega\tau_2, \end{aligned} \tag{2.4}$$

where M_{i1} are analytic functions with $\lim_{\eta\to\pm\infty} M_{i1}(\eta) = M_{i1\pm}$ exist and M_{i2} are nonzero constants (see Appendices A and B). Now we pass to $\eta = \tau_1 - \tau_2$ and τ_2, so we are looking for a simple zero of

$$\begin{aligned} 0 = M_{11}(\eta) + M_{12}\cos\Omega(\eta+\tau_2) &= M_{11}(\eta) + M_{12}(\cos\Omega\eta\cos\Omega\tau_2 - \sin\Omega\eta\sin\Omega\tau_2), \\ M_{21}(\eta) + M_{22}\cos\Omega\tau_2 &= 0. \end{aligned} \tag{2.5}$$

For $\sin\Omega\eta \neq 0$, solving (2.5), we obtain

$$\begin{aligned} \cos\Omega\tau_2 &= -\frac{M_{21}(\eta)}{M_{22}}, \\ \sin\Omega\tau_2 &= \frac{M_{11}(\eta)M_{22} - M_{12}M_{21}(\eta)\cos\Omega\eta}{M_{12}M_{22}\sin\Omega\eta}. \end{aligned} \tag{2.6}$$

By $\cos^2\Omega\tau_2 + \sin^2\Omega\tau_2 = 1$, this yields

$$\begin{aligned} M(\eta) := M_{21}^2(\eta)M_{12}^2\sin^2\Omega\eta + (M_{11}(\eta)M_{22} - M_{12}M_{21}(\eta)\cos\Omega\eta)^2 \\ -M_{12}^2M_{22}^2\sin^2\Omega\eta = 0. \end{aligned} \tag{2.7}$$

For $\sin\Omega\eta = 0$, i.e., $\eta_k = \frac{\pi k}{\Omega}$ for some $k \in \mathbb{Z}$, solving (2.5), we obtain

$$\cos\Omega\tau_2 = -\frac{M_{21}\left(\frac{\pi k}{\Omega}\right)}{M_{22}} \tag{2.8}$$

and

$$M_{11}\left(\frac{\pi k}{\Omega}\right)M_{22} = (-1)^k M_{12}M_{21}\left(\frac{\pi k}{\Omega}\right). \tag{2.9}$$

Lemma 2.1. *A simple root η of (2.7) with $\eta \neq \frac{\pi k}{\Omega}$ for any $k \in \mathbb{Z}$ gives via (2.6) a simple zero of (2.5).*

Proof. Clearly simple zeros of (2.6) are equivalent to simple zeros of (2.5) when $\sin\Omega\eta \neq 0$. Next, we can write (2.6) as

$$\begin{aligned} \cos\Omega\tau_2 - A(\eta) &= 0, \\ \sin\Omega\tau_2 - B(\eta) &= 0 \end{aligned} \tag{2.10}$$

for $A(\eta) = \frac{\widetilde{M}_1(\eta)}{M_3(\eta)}$, $B(\eta) = \frac{\widetilde{M}_2(\eta)}{M_3(\eta)}$, $M_3(\eta) = M_{12}M_{22}\sin\Omega\eta$ and others defined by definition. Then, by (2.7), $M(\eta) = \left(A^2(\eta) + B^2(\eta) - 1\right)M_3^2(\eta)$. The Jacobian of (2.10) at its zero η_0 is

$$\begin{aligned} \Omega\left(A(\eta_0)'\cos\Omega\tau_2 + B(\eta_0)'\sin\Omega\tau_2\right) &= \Omega\left(A(\eta_0)'A(\eta_0) + B(\eta_0)'B(\eta_0)\right) \\ &= \frac{\Omega}{2}\left(A^2(\eta_0) + B^2(\eta_0)\right)' = \frac{\Omega}{2}\left(\frac{M(\eta_0)}{M_3^2(\eta_0)}\right)' = \frac{\Omega M(\eta_0)'}{2M_3^2(\eta_0)}, \end{aligned}$$

since $M(\eta_0) = 0$. Hence any zero of (2.6) is simple if and only if it is generated by a simple root of (2.7). The proof is finished. □

Next, (2.7) is asymptotically near at $\pm\infty$ to

$$\begin{aligned} M_\pm(\eta) &:= M_{21\pm}^2M_{12}^2\sin^2\Omega\eta + (M_{11\pm}M_{22} - M_{12}M_{21\pm}\cos\Omega\eta)^2 - M_{12}^2M_{22}^2\sin^2\Omega\eta \\ &= M_{21\pm}^2M_{12}^2 + M_{11\pm}^2M_{22}^2 - M_{12}^2M_{22}^2 - 2M_{11\pm}M_{22}M_{12}M_{21\pm}\cos\Omega\eta \\ &\quad + M_{12}^2M_{22}^2\cos^2\Omega\eta = 0, \end{aligned} \tag{2.11}$$

where

$$\begin{aligned} M_{11\pm} &= -\int_{-\infty}^{\infty}\frac{9\gamma}{4a^2}\operatorname{sech}^4\frac{z}{2}\tanh^2\frac{z}{2}dz = -\frac{6\gamma}{5a^2}, \\ M_{21\pm} &= \int_{-\infty}^{\infty}\frac{9\gamma}{4a^2}\operatorname{sech}^4\frac{z}{2}\tanh^2\frac{z}{2}dz = \frac{6\gamma}{5a^2}. \end{aligned}$$

Eq. (2.11) has roots

$$\cos\Omega\eta = \frac{-\widetilde{b} \pm \sqrt{\widetilde{b}^2 - 4\widetilde{a}\widetilde{c}}}{2\widetilde{a}} \tag{2.12}$$

for

$$\widetilde{a} = M_{12}^2M_{22}^2, \quad \widetilde{b} = -2M_{11\pm}M_{22}M_{12}M_{21\pm}, \quad \widetilde{c} = M_{21\pm}^2M_{12}^2 + M_{11\pm}^2M_{22}^2 - M_{12}^2M_{22}^2.$$

When

$$\left|\frac{-\widetilde{b}\pm\sqrt{\widetilde{b}^2-4\widetilde{a}\widetilde{c}}}{2\widetilde{a}}\right|<1,$$

i.e.,

$$\left|\gamma^2(\cosh^2\Omega\pi-1)\pm\left(\gamma^2(\cosh^2\Omega\pi-1)-25a^2\Omega^4\pi^2\right)\right|<25a^2\Omega^4\pi^2 \tag{2.13}$$

for either sign, then (2.12) and thus also (2.11) has infinitely many simple roots which gives large (in absolute value) simple roots of (2.7) with $|\cos\Omega\eta|<1$, i.e. $\sin\Omega\eta\neq 0$. For such large η via (2.6), we obtain a simple zero of (2.5). Looking at (2.13), one can see that the inequality is never satisfied for the minus sign. Thus it is equivalent to

$$\gamma\,|\sinh\Omega\pi|<-5a\Omega^2\pi. \tag{2.14}$$

Summarizing we obtain the following result.

Theorem 2.2. *Let $a<0$ and $\beta=0$. Condition (2.14) is sufficient for the persistence of a homoclinic type solution in (2.1) for $\varepsilon\neq 0$ small.*

Finally we do not study the case $\sin\Omega\eta=0$ in more details, since then (2.9) must hold which is rather strong restriction on parameters occurring in (2.1).

2.2. Case (b)

The equations of (2.2) possess heteroclinic solutions

$$p_i=\dot{q}_i,\quad q_i(z)=\tanh\frac{z}{\sqrt{2}}.$$

So in the full space $\mathbb{R}^4$, the system (2.2) has hyperbolic equilibria

$$(\overline{p}_1^{\pm},\overline{q}_1^{\pm},\overline{p}_2^{\pm},\overline{q}_2^{\pm})=(0,\pm1,0,\pm1)$$

connected by the heteroclinic trajectory

$$(p_{1h}(z),q_{1h}(z),p_{2h}(z),q_{2h}(z))=\left(\frac{\operatorname{sech}^2\frac{z}{\sqrt{2}}}{\sqrt{2}},\tanh\frac{z}{\sqrt{2}},\frac{\operatorname{sech}^2\frac{z}{\sqrt{2}}}{\sqrt{2}},\tanh\frac{z}{\sqrt{2}}\right). \tag{2.15}$$

The Melnikov integrals are

$$\begin{aligned}M_1(\tau_1,\tau_2)&=N_{11}(\tau_2-\tau_1)+N_{12}\sin\Omega\tau_1,\\ M_2(\tau_1,\tau_2)&=N_{21}(\tau_2-\tau_1)+N_{22}\sin\Omega\tau_2,\end{aligned} \tag{2.16}$$

where N_{i1} are analytic functions with $\lim_{\eta\to\pm\infty}N_{i1}(\eta)=N_{i1\pm}$ existing and N_{i2} are nonzero constants (see Appendix B). Now taking $\tau_i=\frac{\pi}{2\Omega}-\xi_i$, $i=1,2$, we derive

$$\begin{aligned}N_1(\xi_1,\xi_2)&=M_1\left(\frac{\pi}{2\Omega}-\xi_1,\frac{\pi}{2\Omega}-\xi_2\right)=N_{11}(\xi_1-\xi_2)+N_{12}\cos\Omega\xi_1,\\ N_2(\xi_1,\xi_2)&=M_2\left(\frac{\pi}{2\Omega}-\xi_1,\frac{\pi}{2\Omega}-\xi_2\right)=N_{21}(\xi_1-\xi_2)+N_{22}\cos\Omega\xi_2,\end{aligned}$$

so we can directly apply arguments of case (a) to derive the following result. Of course, instead of (2.7), now we have the function

$$\begin{aligned}N(\eta)=N_{21}^2(\eta)N_{12}^2\sin^2\Omega\eta+(N_{11}(\eta)N_{22}-N_{12}N_{21}(\eta)\cos\Omega\eta)^2\\ -N_{12}^2N_{22}^2\sin^2\Omega\eta=0.\end{aligned} \tag{2.17}$$

Analogously, we derive the condition

$$\left|\frac{-\bar{b}\pm\sqrt{\bar{b}^2-4\bar{a}\bar{c}}}{2\bar{a}}\right|<1 \tag{2.18}$$

with

$$\bar{a}=N_{12}^2N_{22}^2,\quad \bar{b}=-2N_{11\pm}N_{22}N_{12}N_{21\pm},\quad \bar{c}=N_{21\pm}^2N_{12}^2+N_{11\pm}^2N_{22}^2-N_{12}^2N_{22}^2.$$

Putting $\bar{a}, \bar{b}, \bar{c}$ into (2.18), one can see that it is equivalent to

$$\left|\pi^2\Omega^2\operatorname{csch}^2\frac{\Omega\pi}{\sqrt{2}} - 4\left(\pm(\lambda_E+\lambda_E') - \frac{\sqrt{2}\gamma}{3}\right)^2\right| < \pi^2\Omega^2\operatorname{csch}^2\frac{\Omega\pi}{\sqrt{2}},$$

i.e.,

$$0 < \left|\pm(\lambda_E+\lambda_E') - \frac{\sqrt{2}\gamma}{3}\right| < \frac{\Omega\pi}{\sqrt{2}}\operatorname{csch}\frac{\Omega\pi}{\sqrt{2}}. \tag{2.19}$$

Theorem 2.3. *Let $a = 0$ and $\beta = -1$. Condition (2.19) for either sign is sufficient for the persistence of a heteroclinic type solution in (2.1) for $\varepsilon \neq 0$ small.*

3. Numerical results

To illustrate the theoretical results obtained in the previous sections, we have solved the governing equations (1.3) numerically. The advance-delay equation (1.3) is solved using a pseudo-spectral method, i.e., we express the solutions U and V in the trigonometric polynomials

$$\begin{aligned} U(z) &= \sum_{j=1}^{J}\left[A_j\cos\left((j-1)\tilde{k}z\right) + B_j\sin\left(j\tilde{k}z\right)\right], \\ V(z) &= \sum_{j=1}^{J}\left[C_j\cos\left((j-1)\tilde{k}z\right) + D_j\sin\left(j\tilde{k}z\right)\right], \end{aligned} \tag{3.1}$$

where $\tilde{k} = 2\pi/L$ and $-L/2 < z < L/2$. Substituting the series into (1.3) and requiring the representations to satisfy the equations at $2J$ collocation points, we obtain a system of algebraic equations for the Fourier coefficients A_j, B_j, C_j and D_j, $j = 1, 2, \ldots, J$, which are then solved using Newton's method. Typically, we use $L = 30\pi$ and $J = 45$. In the presence of coupling, using the experimentally relevant parameter values provided in [13], in the following we take $\lambda_M' = -0.020$, $\lambda_E' = -0.040$, $\lambda_M = -0.040$ and $\lambda_E = -0.120$.

First, we consider case (a) by taking $a = -1$ and $\beta = 0$. Shown in Fig. 2 is the bifurcation diagram of the localized solution (2.3) for two sets of coupling constants. The vertical axis is the norm defined as

$$Norm = \sqrt{\int_{-L/2}^{L/2} |U(z)|^2 + |V(z)|^2\, dz}.$$

By fixing the driving amplitude ε and varying the gain–loss coefficient γ, we obtain a fold bifurcation. In the figure, we also present the existence boundary, i.e., the fold bifurcation, predicted by our Melnikov function analysis, which is obtained as the following.

In Fig. 3, we plot the function M of (2.7) for two different values of gain–loss parameter, i.e. $\gamma = 0$ and $\gamma = 0.14/\varepsilon$, with $\lambda_M' = -0.020/\varepsilon$, $\lambda_E' = -0.040/\varepsilon$, $\lambda_M = -0.040/\varepsilon$, $\lambda_E = -0.120/\varepsilon$. The division by ε is due to the scaling taken in transforming (1.3) into (2.1). When $\gamma = 0$, we see that the function has many roots. As γ increases, there is a critical value where all the roots become degenerate as shown in panel (b). In Fig. 2, the critical value (multiplied by ε due to the scaling) is depicted as the vertical dashed line, which well predicts the numerical results.

We also consider case (b) by taking $a = 0$ and $\beta = -1$. Shown in Fig. 4 are the bifurcation diagram and the solution profiles. Different from case (a) above, interestingly as the gain–loss coefficient γ varies we obtain a "snaking" profile in the bifurcation diagram, where there are many turning points. This phenomenon is now referred to as homoclinic snaking (see, e.g., [24] and references therein), as it involves homoclinic or heteroclinic structures. In our current case, along the bifurcation diagram, the distance between the kinks increases. The snaking profile appears because of the locking mechanism between the kinks mediated by the oscillating tail that acts as a periodic (i.e. lattice) potential. It is important to note that our Melnikov function (2.17) could predict well the right boundary of the snaking curve. The persistence of the homoclinic snaking as well as the stability of solutions along the bifurcation diagram are beyond the scope of the present paper and will be reported elsewhere.

4. Conclusion

We have investigated localized travelling waves in a chain of PT-symmetric nonlinear metamaterials with gain and loss. We have developed a Melnikov function analysis for detecting the persistence of such waves in the system. By considering two cases of nonlinearity, we compared the theoretical analysis and computational results, where good agreement is obtained. One of the considered cases admits localized waves with a bifurcating diagram exhibiting a "snaking" profile.

The existence and stability of periodic travelling waves (following and extending [25,26] that dealt with only a single advance-delay differential equation), that may be more relevant from applications point of view than travelling localized waves considered herein that most likely are unstable, are addressed for future work.

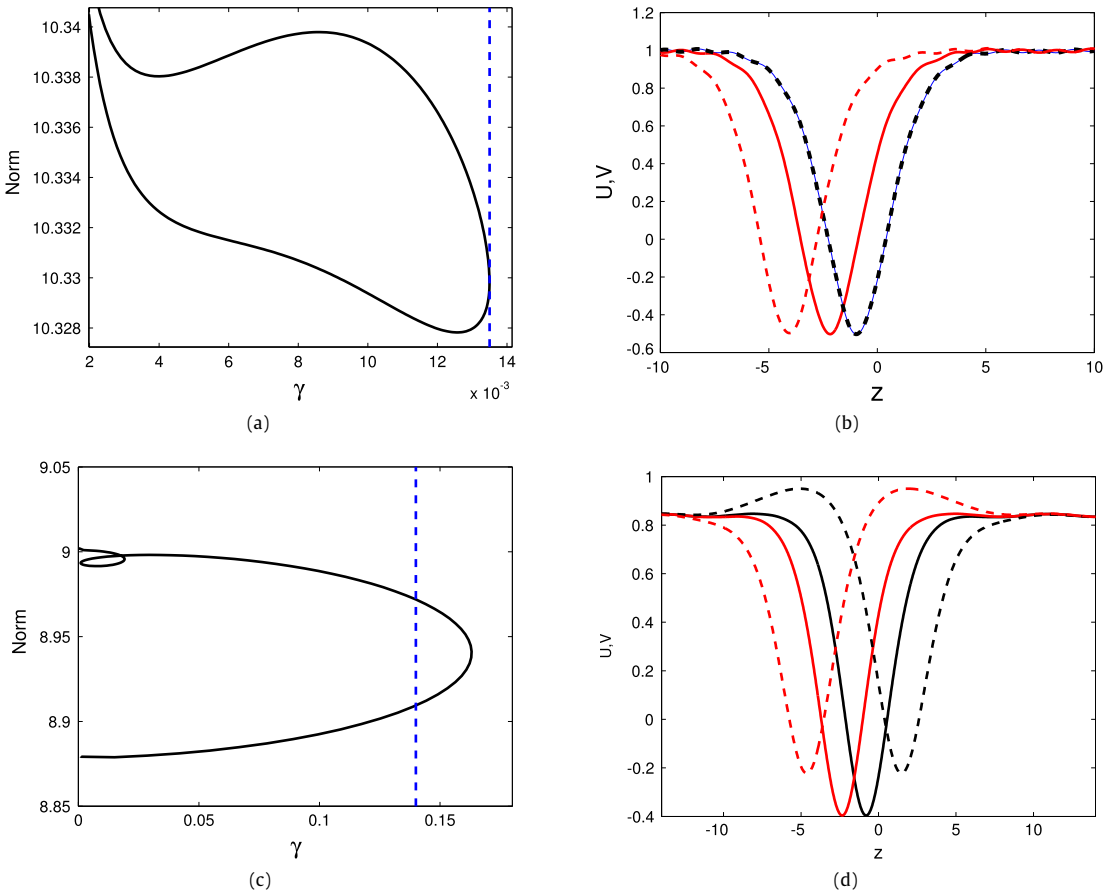

Fig. 2. (a) Bifurcation diagram of the localized solution for $a = -1$, $\beta = 0$, $\lambda'_M = \lambda_M = \lambda'_E = \lambda_E = 0$ and $\varepsilon = 0.01$. The vertical axis is the solution norm and the horizontal axis is the gain–loss coefficient γ. Panel (b) shows the solutions on the lower (solid line) and upper (dashed line) branches at $\gamma = 0.008$. The right and left dips correspond to U and V, respectively. Panels (c,d) are the same as (a,b), but for $\lambda'_M = -0.020$, $\lambda'_E = -0.040$, $\lambda_M = -0.040$, $\lambda_E = -0.120$. Panel (d) shows the solutions at $\gamma = 0.1$. The vertical dashed lines are the existence boundaries given by the Melnikov function.

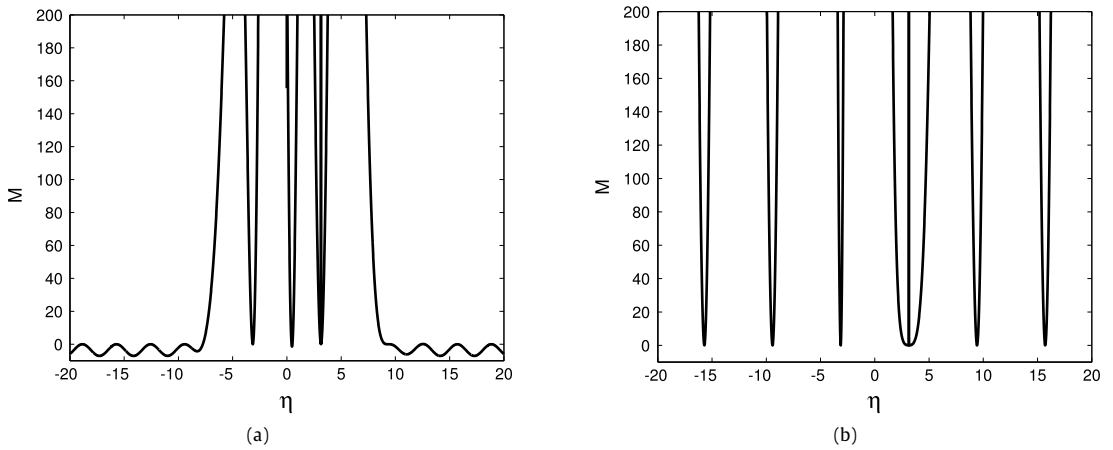

Fig. 3. The Melnikov function M of (2.7) with $\lambda'_M = -0.020/\varepsilon$, $\lambda'_E = -0.040/\varepsilon$, $\lambda_M = -0.040/\varepsilon$, $\lambda_E = -0.120/\varepsilon$ and $\gamma = 0$ (a) or $\gamma = 0.14/\varepsilon$ (b). Here, $\varepsilon = 0.01$.

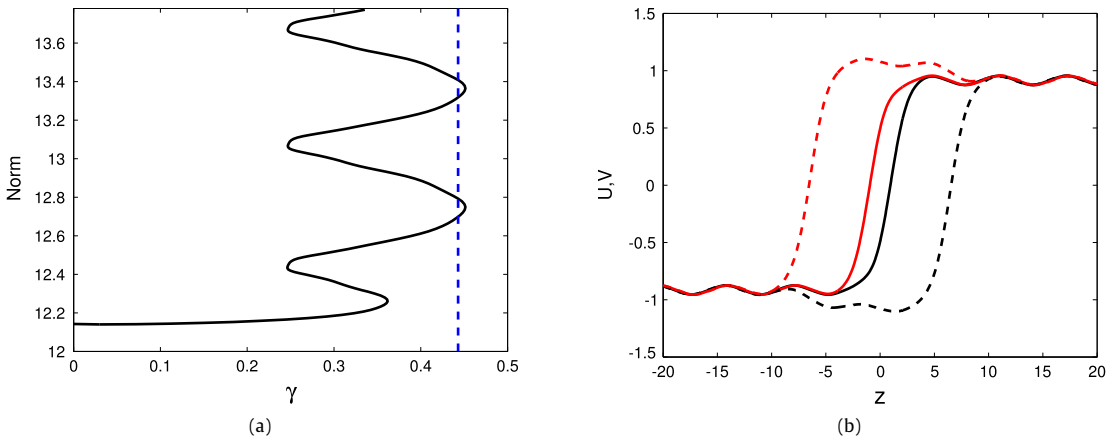

Fig. 4. The same as Fig. 2, but for $a = 0$, $\beta = -1$ and $\varepsilon = 0.1$. Panel (b) shows the solutions for $\gamma = 0.2$ and $\gamma = 0.4$ (at the lowest branch). The right and left kink are U and V, respectively. The vertical dashed line in panel (a) is the approximation obtained from the Melnikov function (2.17).

Acknowledgements

The work of M.A has been co-financed from resources of the operational program "Education and Lifelong Learning" of the European Social Fund and the National Strategic Reference Framework (NSRF) 2007–2013 (2013-ΠΕ2-SHORT TERMS-19736) within the framework of the Action State Scholarships Foundation's (IKY) mobility grants programme for the short term training in recognized scientific/research centres abroad for candidate doctoral or postdoctoral researchers in Greek universities or research centres. M.F. and M.P. were partially supported by the Slovak Grant Agency VEGA No. 2/0153/16 and No. 1/0078/17 and the Slovak Research and Development Agency under the contract No. APVV-14–0378. VR has been co-financed by the European Union (European Social Fund ESF) and Greek national funds through the Operational Program Education and Lifelong Learning of the National Strategic Reference Framework (NSRF) Research Funding Program D.534 MIS:379337: THALES. V.R and M.A acknowledge support from FP7, Marie Curie Actions, People, International Research Staff Exchange Scheme (IRSES-606096). The authors acknowledge the referee for their useful comment and feedback.

Appendix A

The terms in the Melnikov function (2.4) are given by the following integrals

$$
\begin{aligned}
M_{11}(\eta) = &-\int_{-\infty}^{\infty} \frac{9\lambda_M'}{8a^2}\operatorname{sech}^2\frac{z}{2}\tanh\frac{z}{2}\operatorname{sech}^4\frac{z+\eta-p}{2}dz\\
&+\int_{-\infty}^{\infty} \frac{9\lambda_M'}{4a^2}\operatorname{sech}^2\frac{z}{2}\tanh\frac{z}{2}\operatorname{sech}^2\frac{z+\eta-p}{2}\tanh^2\frac{z+\eta-p}{2}dz\\
&-\int_{-\infty}^{\infty} \frac{9\lambda_M}{8a^2}\operatorname{sech}^2\frac{z}{2}\tanh\frac{z}{2}\operatorname{sech}^4\frac{z+\eta}{2}dz\\
&+\int_{-\infty}^{\infty} \frac{9\lambda_M}{4a^2}\operatorname{sech}^2\frac{z}{2}\tanh\frac{z}{2}\operatorname{sech}^2\frac{z+\eta}{2}\tanh^2\frac{z+\eta}{2}dz\\
&-\int_{-\infty}^{\infty} \frac{3\lambda_E'}{2a^2}\operatorname{sech}^2\frac{z}{2}\tanh\frac{z}{2}dz+\int_{-\infty}^{\infty} \frac{9\lambda_E'}{4a^2}\operatorname{sech}^2\frac{z}{2}\tanh\frac{z}{2}\operatorname{sech}^2\frac{z+\eta-p}{2}dz\\
&-\int_{-\infty}^{\infty} \frac{3\lambda_E}{2a^2}\operatorname{sech}^2\frac{z}{2}\tanh\frac{z}{2}dz+\int_{-\infty}^{\infty} \frac{9\lambda_E}{4a^2}\operatorname{sech}^2\frac{z}{2}\tanh\frac{z}{2}\operatorname{sech}^2\frac{z+\eta}{2}dz\\
&-\int_{-\infty}^{\infty} \frac{9\gamma}{4a^2}\operatorname{sech}^4\frac{z}{2}\tanh^2\frac{z}{2}dz\\
&=-\frac{36}{a^2}\left(\lambda_M' I_1(\eta-p)+\lambda_M I_1(\eta)+\lambda_E' I_2(\eta-p)+\lambda_E I_2(\eta)\right)-\frac{6\gamma}{5a^2},
\end{aligned}
$$

$$
M_{12} = -\int_{-\infty}^{\infty}\frac{3}{2a}\operatorname{sech}^2\frac{z}{2}\tanh\frac{z}{2}\sin\Omega z dz = -\frac{6\pi\Omega^2}{a\sinh\Omega\pi},
$$

$$
\begin{aligned}
M_{21}(\eta) = &-\int_{-\infty}^{\infty} \frac{9\lambda_M}{8a^2}\,\mathrm{sech}^2\,\frac{z}{2}\tanh\frac{z}{2}\,\mathrm{sech}^4\,\frac{z-\eta}{2}dz\\
&+\int_{-\infty}^{\infty} \frac{9\lambda_M}{4a^2}\,\mathrm{sech}^2\,\frac{z}{2}\tanh\frac{z}{2}\,\mathrm{sech}^2\,\frac{z-\eta}{2}\tanh^2\frac{z-\eta}{2}dz\\
&-\int_{-\infty}^{\infty} \frac{9\lambda'_M}{8a^2}\,\mathrm{sech}^2\,\frac{z}{2}\tanh\frac{z}{2}\,\mathrm{sech}^4\,\frac{z-\eta+p}{2}dz\\
&+\int_{-\infty}^{\infty} \frac{9\lambda'_M}{4a^2}\,\mathrm{sech}^2\,\frac{z}{2}\tanh\frac{z}{2}\,\mathrm{sech}^2\,\frac{z-\eta+p}{2}\tanh^2\frac{z-\eta+p}{2}dz\\
&-\int_{-\infty}^{\infty} \frac{3\lambda_E}{2a^2}\,\mathrm{sech}^2\,\frac{z}{2}\tanh\frac{z}{2}dz+\int_{-\infty}^{\infty} \frac{9\lambda_E}{4a^2}\,\mathrm{sech}^2\,\frac{z}{2}\tanh\frac{z}{2}\,\mathrm{sech}^2\,\frac{z-\eta}{2}dz\\
&-\int_{-\infty}^{\infty} \frac{3\lambda'_E}{2a^2}\,\mathrm{sech}^2\,\frac{z}{2}\tanh\frac{z}{2}dz+\int_{-\infty}^{\infty} \frac{9\lambda'_E}{4a^2}\,\mathrm{sech}^2\,\frac{z}{2}\tanh\frac{z}{2}\,\mathrm{sech}^2\,\frac{z-\eta+p}{2}dz\\
&+\int_{-\infty}^{\infty} \frac{9\gamma}{4a^2}\,\mathrm{sech}^4\,\frac{z}{2}\tanh^2\frac{z}{2}dz\\
=&-\frac{36}{a^2}\left(\lambda_M I_1(-\eta)+\lambda'_M I_1(-\eta+p)+\lambda_E I_2(-\eta)+\lambda'_E I_2(-\eta+p)\right)+\frac{6\gamma}{5a^2},
\end{aligned}
$$

$$
M_{22} = -\int_{-\infty}^{\infty} \frac{3}{2a}\,\mathrm{sech}^2\,\frac{z}{2}\tanh\frac{z}{2}\sin\Omega z dz = -\frac{6\pi\Omega^2}{a\sinh\Omega\pi}
$$

where

$$
I_1(z) = \frac{(5+50\mathrm{e}^z-50\mathrm{e}^{3z}-5\mathrm{e}^{4z}+z(1+26\mathrm{e}^z+66\mathrm{e}^{2z}+26\mathrm{e}^{3z}+\mathrm{e}^{4z}))\mathrm{e}^z}{(1-\mathrm{e}^z)^6},
$$

$$
I_2(z) = \frac{(3-3\mathrm{e}^{2z}+z(1+4\mathrm{e}^z+\mathrm{e}^{2z}))\mathrm{e}^z}{(1-\mathrm{e}^z)^4}.
$$

Appendix B

The integral terms in (2.16) are given by

$$
\begin{aligned}
N_{11}(\eta) = &\int_{-\infty}^{\infty} \frac{\lambda'_M}{\sqrt{2}}\,\mathrm{sech}^2\,\frac{z}{\sqrt{2}}\,\mathrm{sech}^2\,\frac{z-\eta-p}{\sqrt{2}}\tanh\frac{z-\eta-p}{\sqrt{2}}dz\\
&+\int_{-\infty}^{\infty} \frac{\lambda_M}{\sqrt{2}}\,\mathrm{sech}^2\,\frac{z}{\sqrt{2}}\,\mathrm{sech}^2\,\frac{z-\eta}{\sqrt{2}}\tanh\frac{z-\eta}{\sqrt{2}}dz\\
&-\int_{-\infty}^{\infty} \frac{\lambda_E}{\sqrt{2}}\,\mathrm{sech}^2\,\frac{z}{\sqrt{2}}\tanh\frac{z-\eta}{\sqrt{2}}dz-\int_{-\infty}^{\infty} \frac{\gamma}{2}\,\mathrm{sech}^4\,\frac{z}{\sqrt{2}}dz\\
&-\int_{-\infty}^{\infty} \frac{\lambda'_E}{\sqrt{2}}\,\mathrm{sech}^2\,\frac{z}{\sqrt{2}}\tanh\frac{z-\eta-p}{\sqrt{2}}dz\\
=&\,8\left(\lambda'_M J_1(-\eta-p)+\lambda_M J_1(-\eta)\right)+2\left(\lambda'_E J_2(-\eta-p)+\lambda_E J_2(-\eta)\right)-\frac{2\sqrt{2}\gamma}{3},
\end{aligned}
$$

$$
N_{12} = \int_{-\infty}^{\infty} \frac{1}{\sqrt{2}}\,\mathrm{sech}^2\,\frac{z}{\sqrt{2}}\cos\Omega z dz = \sqrt{2}\pi\Omega\,\mathrm{csch}\,\frac{\Omega\pi}{\sqrt{2}},
$$

$$
\begin{aligned}
N_{21}(\eta) = &\int_{-\infty}^{\infty} \frac{\lambda_M}{\sqrt{2}}\,\mathrm{sech}^2\,\frac{z}{\sqrt{2}}\,\mathrm{sech}^2\,\frac{z+\eta}{\sqrt{2}}\tanh\frac{z+\eta}{\sqrt{2}}dz\\
&+\int_{-\infty}^{\infty} \frac{\lambda'_M}{\sqrt{2}}\,\mathrm{sech}^2\,\frac{z}{\sqrt{2}}\,\mathrm{sech}^2\,\frac{z+\eta+p}{\sqrt{2}}\tanh\frac{z+\eta+p}{\sqrt{2}}dz\\
&-\int_{-\infty}^{\infty} \frac{\lambda_E}{\sqrt{2}}\,\mathrm{sech}^2\,\frac{z}{\sqrt{2}}\tanh\frac{z+\eta}{\sqrt{2}}dz-\int_{-\infty}^{\infty} \frac{\lambda'_E}{\sqrt{2}}\,\mathrm{sech}^2\,\frac{z}{\sqrt{2}}\tanh\frac{z+\eta+p}{\sqrt{2}}dz\\
&+\int_{-\infty}^{\infty} \frac{\gamma}{2}\,\mathrm{sech}^4\,\frac{z}{\sqrt{2}}dz\\
=&\,8\left(\lambda_M J_1(\eta)+\lambda'_M J_1(\eta+p)\right)+2\left(\lambda_E J_2(\eta)+\lambda'_E J_2(\eta+p)\right)+\frac{2\sqrt{2}\gamma}{3},
\end{aligned}
$$

$$N_{22} = \int_{-\infty}^{\infty} \frac{1}{\sqrt{2}} \operatorname{sech}^2 \frac{z}{\sqrt{2}} \cos \Omega z dz = \sqrt{2}\pi\,\Omega \operatorname{csch} \frac{\Omega\pi}{\sqrt{2}}$$

where

$$J_1(z) = \frac{\left(3 - 3\mathrm{e}^{2\sqrt{2}z} + \sqrt{2}z\left(1 + 4\mathrm{e}^{\sqrt{2}z} + \mathrm{e}^{2\sqrt{2}z}\right)\right)\mathrm{e}^{\sqrt{2}z}}{(1 - \mathrm{e}^{\sqrt{2}z})^4},$$

$$J_2(z) = \frac{1 - \mathrm{e}^{2\sqrt{2}z} + 2\sqrt{2}z\mathrm{e}^{\sqrt{2}z}}{(1 - \mathrm{e}^{\sqrt{2}z})^2},$$

and

$$\begin{aligned} N_{11\pm} &= \pm \int_{-\infty}^{\infty} \frac{\lambda_E + \lambda_E'}{\sqrt{2}} \operatorname{sech}^2 \frac{z}{\sqrt{2}} dz - \int_{-\infty}^{\infty} \frac{\gamma}{2} \operatorname{sech}^4 \frac{z}{\sqrt{2}} dz \\ &= \pm 2(\lambda_E + \lambda_E') - \frac{2\sqrt{2}\gamma}{3}, \\ N_{21\pm} &= \mp \int_{-\infty}^{\infty} \frac{\lambda_E + \lambda_E'}{\sqrt{2}} \operatorname{sech}^2 \frac{z}{\sqrt{2}} dz + \int_{-\infty}^{\infty} \frac{\gamma}{2} \operatorname{sech}^4 \frac{z}{\sqrt{2}} dz \\ &= \mp 2(\lambda_E + \lambda_E') + \frac{2\sqrt{2}\gamma}{3}. \end{aligned}$$

References

[1] J.B. Pendry, A.J. Holden, W.J. Stewart, Extremely low frequency plasmons in metallic microstructures, Phys. Rev. Lett. 76 (1996) 4773—4776.
[2] J.B. Pendry, A.J. Holden, W.J. Stewart, Magnetism from conductors and enhanced nonlinear phenomena, IEEE Trans. Microwave Theory Techn. 47 (1999) 2075—2084.
[3] V.G. Veselago, The electrodynamics of substances with simultaneously negative values of ϵ and μ, Sov. Phys. Uspekhi 10 (1968) 509—514.
[4] D.R. Smith, W.J. Padilla, D.C. Vier, S.C. Nemat-Nasser, S. Schultz, Composite medium with simultaneously negative permeability and permittivity, Phys. Rev. Lett. 84 (2000) 4184—4187.
[5] C.M. Bender, D.D. Holm, D.W. Hook, Complexified dynamical systems, J. Phys. A: Math. Theor. 40 (2007) F793.
[6] R. El-Ganainy, K.G. Makris, D.N. Christodoulides, Z.H. Musslimani, Theory of coupled optical PTsymmetricstructures, Opt. Lett. 32 (2007) 2632.
[7] K.G. Makris, R. El-Ganainy, D.N. Christodoulides, Z.H. Musslimani, Beam dynamics in PT symmetric optical lattices, Phys. Rev. Lett. 100 (2008) 103904.
[8] S.V. Dmitriev, A.A. Sukhorukov, Yu.S. Kivshar, Binary parity-time-symmetric nonlinear lattices with balanced gain and loss, Opt. Lett. 35 (2010) 2976.
[9] N. Lazarides, G.P. Tsironis, Phys. Rev. Lett. 110 (2013) 053901.
[10] O. Sydoruk, A. Radkovskaya, O. Zhuromskyy, E. Shamonina, M. Shamonin, C.J. Stevens, G. Faulkner, D.J. Edwards, L. Solymar, Tailoring the near-field guiding properties of magnetic metamaterials with two resonant elements per unit cell, Phys. Rev. B 73 (2006) 224406.
[11] F. Hesmer, E. Tatartschuk, O. Zhuromskyy, A.A. Radkovskaya, M. Shamonin, T. Hao, C.J. Stevens, G. Faulkner, D.J. Edwards, E. Shamonina, Coupling mechanisms for split ring resonators: Theory and experiment, Phys. Status Solidi (b) 244 (2007) 1170.
[12] I. Sersic, M. Frimmer, E. Verhagen, A.F. Koenderink, Electric and magnetic dipole coupling in near-infrared split-ring metamaterial arrays, Phys. Rev. Lett. 103 (2009) 213902.
[13] N.N. Rosanov, N.V. Vysotina, A.N. Shatsev, I.V. Shadrivov, D.A. Powell, Y.S. Kivshar, Discrete dissipative localized modes in nonlinear magnetic metamaterials, Opt. Express 19 (27) (2011) 26500—26506.
[14] N. Feth, M. Konig, M. Husnik, K. Stannigel, J. Niegemann, K. Busch, M. Wegener, S. Linden, Electromagnetic interaction of spit-ring resonators: The role of separation and relative orientation, Opt. Express 18 (2010) 6545–6554.
[15] N. Lazarides, M. Eleftheriou, G.P. Tsironis, Discrete breathers in nonlinear magnetic metamaterials, Phys. Rev. Lett. 97 (2006) 157406.
[16] N. Lazarides, V. Paltoglou, G.P. Tsironis, Nonlinear magnetoinductive transmission lines, Int. J. Bifurcation Chaos 21 (2011) 2147.
[17] M.I. Molina, N. Lazarides, G.P. Tsironis, Bulk and surface magnetoinductive breathers in binary metamaterials, Phys. Rev. E 80 (2009) 046605.
[18] J. Diblík, M. Fečkan, M. Pospíšil, V.M. Rothos, H. Susanto, Localized excitations in nonlinear complex systems, Nonlinear Syst. Complex. 7 (2014) 335–358.
[19] M. Fečkan, M. Pospíšil, H. Susanto, Bifurcation of travelling waves in implicit nonlinear lattices: Applications in metamaterials, Appl. Anal. 96 (2017) 578–589.
[20] S. Wiggins, Global Bifurcations and Chaos—Analytical Methods, Springer-Verlag, New York, 1988.
[21] S. Wiggins, Global Dynamics, Phase Space Transport, Orbits Homoclinic To Resonances, and Applications, in: Field Institute Monographs, vol. 1, AMS, Providence, USA, 1993.
[22] K. Yagasaki, The method of Melnikov for perturbations of multi-degree-of-freedom Hamiltonian systems, Nonlinearity 12 (1999) 799–822.
[23] K. Yagasaki, Periodic and homoclinic motions in forced, coupled oscillators, Nonlinear Dynam. 20 (1999) 319—359.
[24] P.C. Matthews, H. Susanto, Variational approximations to homoclinic snaking in continuous and discrete systems, Phys. Rev. E 84 (2011) 066207–066211.
[25] M. Fečkan, M. Pospíšil, V.M. Rothos, H. Susanto, Periodic travelling waves of forced FPU lattices, J. Dyn. Diff. Equat. 25 (2013) 795–820.
[26] M. Agaoglou, M. Fečkan, M. Pospíšil, V.M. Rothos, H. Susanto, Travelling waves in nonlinear magneto-inductive lattices, J. Differ. Equ. 260 (2016) 1717–1746.